FPGA-based Multi-parametric Non-linear Model Predictive Control for a Micro-Grid in Small Islands

H. K. Mudaliar*, D. M.Kumar*, S. Rokocakau*, K. Ram*, M. Assaf*, M. Cirrincione*, and A. Mohammadi*
(*) School of Engineering and Physics, The University of the South Pacific, Laucala Campus, Suva, Fiji.
Contact author email: cirrincione_m@usp.ac.fj

Abstract - This paper studies the concept of Non-linear Predictive Control (NMPC) to micro-grid in remote small islands in Fiji or the Pacific region. A multi-parametric model with a suitable cost function is considered for a micro-grid supplied by renewable energy sources and with a fly-wheel energy storage system The proposed control strategy has been designed for implementation on an Field-Programmable gate array (FPGA) board, for its the great advantages of reducing the overall system cost, size, and real-time operation, making it suitable for easy and cheap application in small islands or villages.

I. INTRODUCTION

Climate change has brought several challenges to developing island nations. In the South Pacific region, countries face a unique energy challenge coupled with oil price vulnerability. Research has indicated that the GDP of a Pacific Island Country (PIC) can drop by as much as 1.5% for a price increase of just 10 dollars per barrel [1]. The need for cleaner sources of power generation results in the use of Renewable Energy Sources (RES) especially in micro-grids, particularly suitable for powering small islands or areas not connected with the main grid in PICs.

Overall, micro-grids typically have two modes of operation, standalone (islanded) and grid connected mode and can change between these modes [2], [3]. Micro-grids provide voltage and frequency regulation support and improve reliability and power capacity [4]. However, one of the challenges for micro-grids is the need to control and balance a large number of generation sources and loads amidst resource uncertainty and constraints. In this respect, there are several important factors to consider in micro-grid control: voltage and current control, power sharing among distributed energy resources, demand side management, optimal economic dispatch as well as transition between grid connected and standalone modes [5], [6]. Due to the uncertainty in RES, the generation profile of the micro-grid is always uncertain and highly constrained. Moreover, load profiles may be predictable to a higher certainty only for small communities with mostly residential energy use. All of these factors, together with the necessity of meeting the different constraints in terms of voltage and currents as well as loss minimization and others associated to the different devices of a micro-grid, make the use of traditional PI control with limiters not suitable and difficult to achieve. One natural solution is the use of the Model Predictive Control (MPC) with constraints, which inherently generates control actions while simultaneously meeting the constraints. Indeed, MPC is a model-based design technique that is a special case of optimal control techniques [7]. Several algorithms for MPC have been proposed in literature both for linear a nonlinear systems [8], [9] so that constraints over the control actions and the state variables are satisfied while minimizing a suitable cost function. Thus, systematic approaches for solving the optimization problem have been developed [10] . However, these methods theoretically result in algorithms computationally cumbersome and do not consider practical hardware and real time implementations.

A decentralized model predictive control strategy designed to control the modules of an integrated power system (IPS) based on fuel cell (FC), battery, photovoltaic panels (PV), and two diesel generators is proposed in [11]. This method is based on a hierarchical structure with virtual droop control and power management strategy and computer simulation results show good response and stability in various operational load conditions. A survey of the discrete form of the model predictive control in electrical drive systems is discussed in [12], where several finite control set model predictive control algorithms are introduced and compared with conventional control strategies for electric drives. A fixed switching frequency scheme for finite-control-set model predictive control is presented in [13], where the proposed method is capable of achieving an output waveform quality comparable to that of a pulse-width-modulator-based linear controller. A good reference about the application of finite set MPC is [14], where it is applied to the control of electrical drives and inverters. The concept is validated by applying it to a five-level flying-capacitor converter. In [15] a classic gradient method in fixed-point arithmetic is used to propose a numerically stable field-programmable gate array (FPGA) implementation for the complex model predictive pulse pattern controller. It is shown that the proposed FPGA implementation improves the performance in terms of speed by as much as ten times and a resource reduction by as much as 17 times for the case of three transitions per phase as compared to other solutions. However, no paper addresses the application of predictive control to small micro-grids that could possibly be developed in small islands like those in the Pacific, considering the reduced load demands of the village and the need of a cheap implementation.

In this respect this work aims to fill this gap addressing the application of a finite state predictive control for a small micro-grid not connected to the main grid, as is the case for most islands in the Pacific region. The considered case is a micro-grid powered by photovoltaic panels (PV), with a fly-wheel energy storage system (FESS), and mostly residential loads. The idea is, therefore, to propose the design of a simplified predictive algorithm to be implemented in a low-cost FPGA, so as to make it affordable for small villages.

The paper is organized as follows. Section II presents the methodology. Section III describes the MPC adopted and the embedded processor design and finally Section IV shows the results.

II. METHODOLOGY

This paper proposes a Predictive Torque Control (PTC) algorithm, as described in [14], together with PIs to control a

Copyright ⓒ KIEE Electrical Machinery and Energy Conversion Systems

small micro-grid not connected to the grid, composed of PVs for energy supply in conjunction with a FESS. The algorithm minimizes the oscillations of the DC-link while controlling in torque the FESS.
The FESS is made up of an induction motor drive connected to a fly-wheel. In order to simplify the algorithm, the MPC has been limited only to the PTC of the FESS, by minimizing a cost function dependent on the torque reference and the flux reference for the electrical drive.

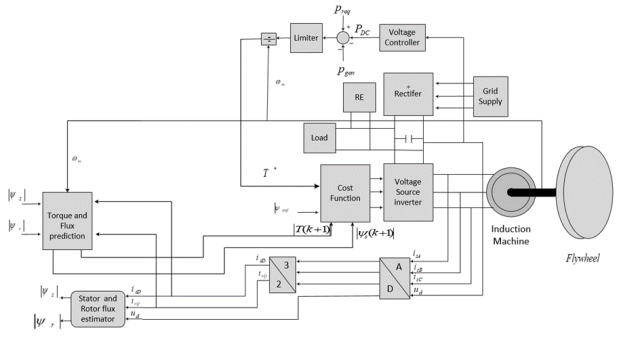

Figure 1: Predictive control scheme

Fig.1 shows how a FESS is used to regulate the DC-Link voltage and the power flow in the micro-grid. To regulate the DC-Link voltage, a PI compensator is introduced whose output is the necessary power (P_{DC}) required to regulate the DC-Link voltage to the reference value V_{DCref}. If P_{req} is the power exchanged with the FESS (positive if it flows towards the DC-link), and P_{gen} is the power generated by RES (and the grid if it is connected) and injected into the DC-link node, then the reference power that needs to be produced by the FESS is given by the equation:

$$P_{ref} = P_{req} - P_{gen} - P_{DC} \quad (1)$$

From the above equation the reference torque that is needed for the PTC is given by the equation,

$$T^* = \frac{P_{ref}}{\omega_m} + T_{FW} \quad (2)$$

Where $\omega_m$is the fly-wheel speed $[rad/s]$, and T_{FW} is the torque of the fly-wheel (which depends on the speed). It should be noted that the value of P_{ref} must not exceed the maximum power of the induction motor. The DC-link is connected with PVs and the load.
The estimation (indicated below by ^) of the stator flux flux-linkage is derived from the discretization of stator voltage equation given below:

$$\hat{\boldsymbol{\psi}}_s(k) = \hat{\boldsymbol{\psi}}_s(k-1) + T_s \boldsymbol{v}_s(k) - R_s T_s \boldsymbol{i}_s(k) \quad (3)$$

where $\boldsymbol{v}_s$ is stator space-vector voltage, R_s is stator resistance, $\boldsymbol{i}_s$ is stator space-vector current and $\boldsymbol{\psi}_s$ is the stator flux-linkage space-vector, T_s is the sampling period, k the discrete time.
Similarly the rotor flux-linkage is computed as:

$$\hat{\boldsymbol{\psi}}_r(k) = \frac{L_r}{L_m} \hat{\boldsymbol{\psi}}_s(k) + \boldsymbol{i}_s(k)\left(L_m - \frac{L_r L_s}{L_m}\right) \quad (4)$$

where $\boldsymbol{\psi}_r$ is the rotor flux linkage space-vector, L_m is the mutual inductance, L_r is the rotor inductance and L_s is the stator inductance. The eq.s (3) and (4) are implemented in the block "stator and rotor estimation" of Fig.1.
The block "torque and flux prediction" implements a one-step prediction of the FESS by using the formulas (5) and (6), where the apex p indicates the predicted variable:

$$\hat{\boldsymbol{\psi}}_s^{\boldsymbol{p}}(k+1) = \hat{\boldsymbol{\psi}}_s(k) + T_s \boldsymbol{v}_s(k) - R_s T_s \boldsymbol{i}_s(k) \quad (5)$$

$$T^p(k+1) = \frac{3}{2} P \; Im\{\bar{\boldsymbol{\psi}}_s^{\boldsymbol{p}}(k+1) \boldsymbol{i}_s^{\boldsymbol{p}}(k+1)\} \quad (6)$$

P indicates the number of pair-poles, and T is the electromagnetic torque and $\boldsymbol{i}_s^{\boldsymbol{p}}(k+1)$ is the predicted stator current space-vector, given by (7):

$$\boldsymbol{i}_s^{\boldsymbol{p}}(\boldsymbol{k+1}) = \left(1 + \frac{T_s}{\tau_\sigma}\right) \boldsymbol{i}_s(\boldsymbol{k}) + \frac{T_s}{\tau_\sigma + T_s}\left\{\frac{1}{R_\sigma}\left[\left(\frac{k_r}{\tau_r} - k_r j\omega\right) \hat{\boldsymbol{\psi}}_r(k) + \boldsymbol{v}_s(k)\right]\right\} \quad (7)$$

See Appendix 1 for the definition of the parameters in (7).
Both the stator flux and electromagnetic torque predictions are written in terms of the inverter voltage, $\boldsymbol{v}_s(k)$, implying eight different predictions for both the torque and flux, $(T^p(k+1), \psi_s{}^p(k+1))_h$, $h \in [0,1,2,\ldots\ldots,7]$ according to the number of voltage vectors generated by the two-level inverter. $\boldsymbol{i}_s(\boldsymbol{k})$ is the measured current.

In obtaining the switching state selection, a cost function containing the control law is used to compare the torque and flux references with the predicted values, evaluating for every prediction the one producing the lowest value. The corresponding firing pulses are generated for the two level inverter. The cost function is as defined in (8):

$$g_h = |T^* - T^p(k+1)_h| + \lambda \left|\psi_s^* - \psi_s^p(k+1)_h\right| \quad (8)$$

where λ is a suitable weighting factor.

III. PREDICTIVE CONTROL ALGORITHM & EMBEDDED PROCESSOR DESIGN

Computer simulations have been developed in MATLAB/SIMULINK® to prove the concept, validate the proposed theoretical strategy and demonstrate its effectiveness. The final algorithm is designed as an embedded processor to be implemented in HDL hardware language [15] on an FPGA board [16].
Fig.2 shows the predictive torque control topology which is designed to be implemented on an FPGA board. In Fig.2 ω^* is the speed reference, $|\psi_r{}^*|$ is the rotor flux reference, v_s is the stator voltage, $i_s$is the stator current and T is the electromagnetic torque.
The design of the controller as an Application Specific Instruction Set Embedded Processor (ASIP) is presented below. The embedded processor design can be implemented in hardware on a VLSI chip or on an FPGA board for fast prototyping.

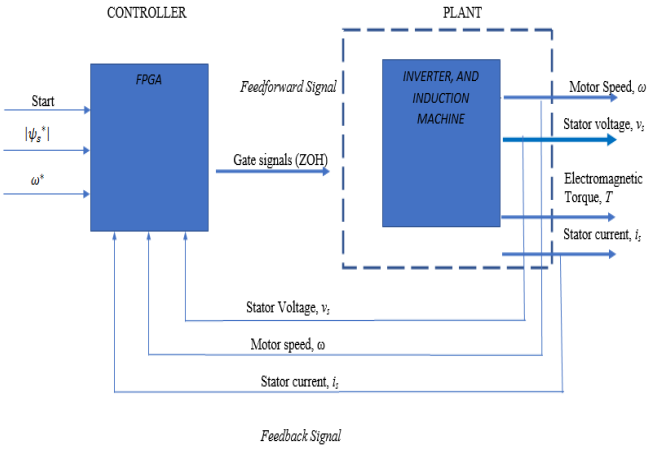

Figure 2 - Predictive Torque Control high-level Architecture

Figure 3 depicts the Finite State Machine with Datapath (FSMD) of the control algorithm, in which instructions and data are represented by separate states.

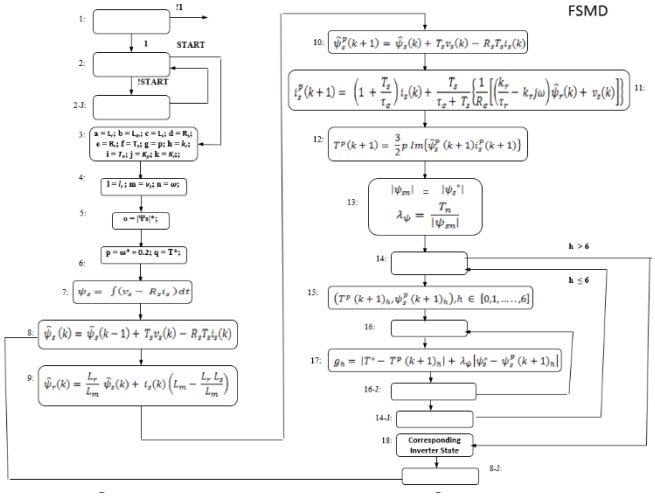

Figure 4 shows the design of the controller, where data and constant parameters are replaced by registers, while instructions are replaced by control signals. Individual states are assigned unique binary identifiers.

Input control signals such as dat_sel, a_ld, b_ld, ALUs, Mre, and Mwe are sent out by the controller to configure the logic represented by the datapath and the memory.

Output control signals such as ALUz are feedback signals returned by the datapath to the controller to indicate the status of execution of operations, as shown in figure 5.

The overall design consist of a control logic and state register unit (controller), a program counter (PC), instruction register (IR), multiplexer to route memory addresses, program memory, data memory, register bank, and custom arithmetic and logic unit (custom ALU) capable of performing digital signal processing and floating point operations. Multiple custom ALU's can be used to perform parallel computation in terms of the predicted states of the algorithm. In the next section simulation results are presented.

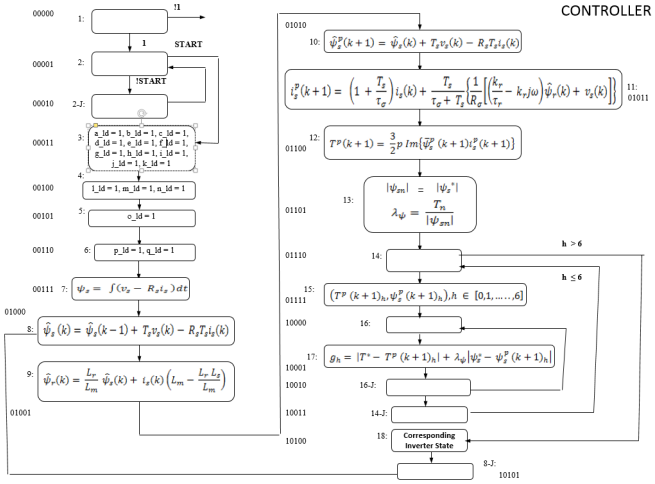

Figure 4 – Controller design

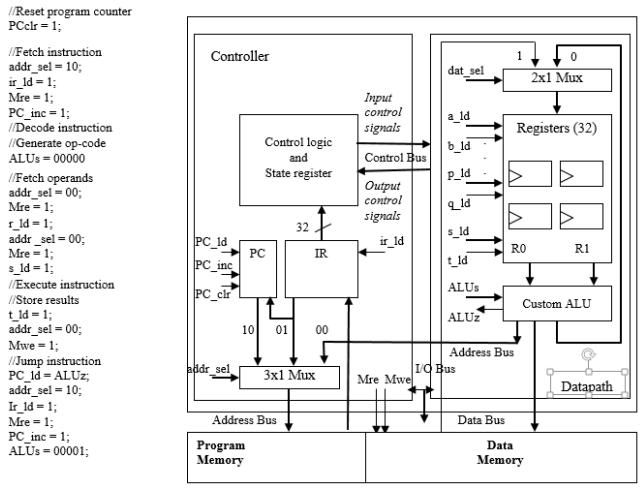

Figure 5 – Combined controller and datapath design

IV. RESULTS

The simulation results of control algorithm for a micro-grid in a small island with PVs and a FESS with the load of a typical Fiji village are shown in Fig.s 6 to 10. A typical load for a small village of about 10 households is about 2 kW, mostly for lighting, TV and one fridge [17]. Fig. 6 shows the evolution of the load in 10s.

In the first scenario i.e. from time interval 21s to 24s the FESS is commanded by the PTC to ramp up its speed above its reference speed from 262 rad/s to 270 rad/s as shown in Fig. 7. This change in speed occurs because the generation from the RES is greater than the local load demand as shown in Fig. 6 and 9, depicting this the intermittent PV energy provided. Thus, the excess energy from the RES is absorbed by the FESS as shown in Fig. 10 keeping the DC link voltage constant at 700 V_{DC} as shown in Fig. 8. A similar scenario can be seen at time interval of 26 seconds to 28 seconds

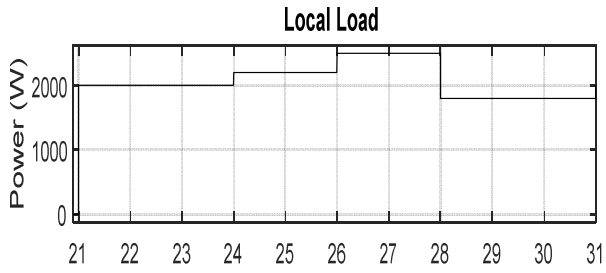

Figure 6 - Local small island load

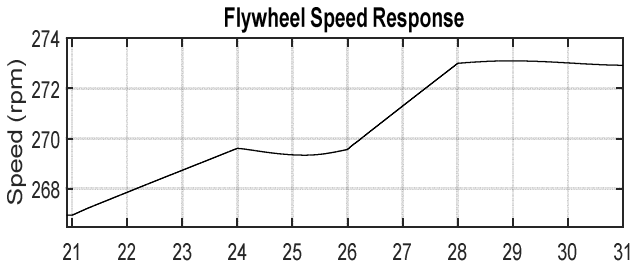

Figure 7 - Speed response of Flywheel coupled with induction motor

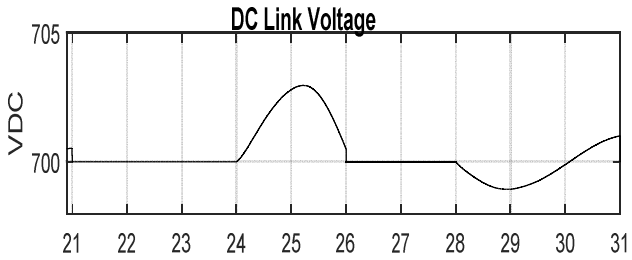

Figure 8- DC link voltage of them micro-grid

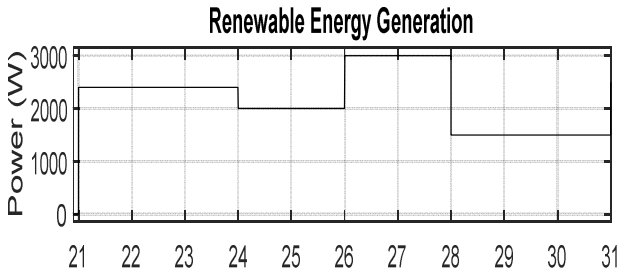

Figure 9 - Renewable energy generation by PV array

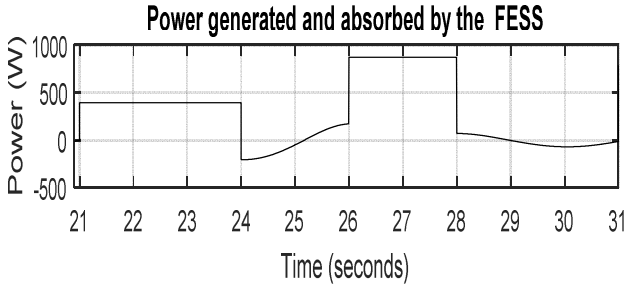

Figure 6 - Power generated and absorbed by Flywheel

In the second scenario appears from time interval 24s to 26s when the FESS speed starts to decrease from 270 rad/s. This change in speed of the FESS occurs because the local load demand is greater than the RES generation as shown in Fig. 6 and 9. In this case, the rotating energy stored in the FESS is used to compensate the deficit energy required by the local load as shown in Fig. 10. A similar scenario can be seen at time interval 28s to 31s.

V. CONCLUSION

This paper proposes the design and implementation of PTC algorithm as an application specific instruction set processor suitable for deployment of the FESS on remote islands. The embedded processor offers the great advantages of reducing the overall system cost, size, and real-time operation. Parallel computation can be performed to increase the overall speedup of the system. In the future real-time hardware verification of the control algorithm on a ASIP is to be carried out.

The proposed approach suggests that, if FESS were introduced in micro-grids situated in remote islands, the use of batteries could be minimized. Actually, batteries have a shorter life term, disposal issues, high maintenance cost, whereas FESS have a longer life span and rarely needs maintenance. Thus, the use of FESS is highly recommended for remote islands. Furthermore, to reduce the overall system cost, reduce size, and increase performance this work proposes the ASIP design of the processor to be implemented on a FPGA board. The FPGA programming offers flexibility as microprocessor parameters can be tuned to the application with tight on-chip interconnection with additional circuitry. Finally, once the design is validated on FPGA board then it can be sent for fabrication on a VLSI chip.

References

[1] T. Banuri, “Trends in Sustainable Development; Small Island Developing States,” Div. Sustain. Dev., 2010.

[2] A. Hirsch, Y. Parag, and J. Guerrero, “Microgrids: A review of technologies, key drivers, and outstanding issues,” Renew. Sustain. Energy Rev., vol. 90, pp. 402–411, Jul. 2018.

[3] D. T. Ton and M. A. Smith, “The U.S. Department of Energy’s Microgrid Initiative,” Electr. J., vol. 25, no. 8, pp. 84–94, Oct. 2012.

[4] A. Llaria, O. Curea, J. Jiménez, and H. Camblong, “Survey on microgrids: Unplanned islanding and related inverter control techniques,” Renew. Energy, vol. 36, no. 8, pp. 2052–2061, Aug. 2011.

[5] D. E. Olivares et al., “Trends in Microgrid Control,” IEEE Trans. Smart Grid, vol. 5, no. 4, pp. 1905–1919, Jul. 2014.

[6] W. C. Clarke, C. Manzie, and M. J. Brear, “An economic MPC approach to microgrid control,” in 2016 Australian Control Conference (AuCC), 2016, pp. 276–281.

[7] M. Morari and J. H. Lee, “Model predictive control: past, present and future,” Comput. Chem. Eng., vol. 23, no. 4, pp. 667–682, May 1999.

[8] Jan Maciejowski., Predictive Control with Constraints", Pearson Education, ISBN: 0-201-39823-0, 331 pages, June 2001, Prentice Hall.
[9] A. Parisio and L. Glielmo, "Stochastic Model Predictive Control for economic/environmental operation management of microgrids," in 2013 European Control Conference (ECC), 2013, pp. 2014–2019.
[10] S. L. de O. Kothare and M. Morari, "Contractive model predictive control for constrained nonlinear systems," IEEE Trans. Autom. Control, vol. 45, no. 6, pp. 1053–1071, Jun. 2000.
[11] M. R. Banaei and R. Alizadeh, "Simulation-Based Modeling and Power Management of All-Electric Ships Based on Renewable Energy Generation Using Model Predictive Control Strategy," IEEE Intell. Transp. Syst. Mag., vol. 8, no. 2, pp. 90–103, Summer 2016.
[12] F. Wang, X. Mei, J. Rodriguez, and R. Kennel, "Model predictive control for electrical drive systems-an overview," CES Trans. Electr. Mach. Syst., vol. 1, no. 3, pp. 219–230, Sep. 2017.
[13] M. Tomlinson, H. d T. Mouton, R. Kennel, and P. Stolze, "A Fixed Switching Frequency Scheme for Finite-Control-Set Model Predictive Control #8212;Concept and Algorithm," IEEE Trans. Ind. Electron., vol. 63, no. 12, pp. 7662–7670, Dec. 2016.
[14] Jose Rodriguez, Patricio Cortes," Predictive Control of Power Converters and Electrical Drives", ISBN: 978-1-119-96398-1, 246 pages, April 2012, Wiley-IEEE Press
[15] HDL Coder: Getting Started Guide. MathWorks, March 2012.
[16] S. Jose, "Cyclone IV Device Handbook, Volume 3," vol. 3, p. 54, 2016.
[17] D. Aitchison, M. Cirrincione, G. Cirrincione, A. Mohammadi, M. Pucci "Feasibility Study and Design of a Flywheel Energy System in a Microgrid for Small Village in Pacific Island State Countries", Chapter 6 in: Smart Energy Grid Design for Island Countries Challenges and Opportunities, pp.159-187, Springer, May 2017, Print ISBN: 978-3-319-50196-3, Electronic ISBN: 978-3-319-50197-0

Appendix 1

$$\tau_\sigma = \frac{\sigma L_s}{R_\sigma}$$

$$\sigma = 1 - \frac{L_m^2}{L_s L_r}$$

$$\tau_r = \frac{L_r}{R_r}$$

$$k_r = \frac{L_m}{L_r}$$

$$R_\sigma = R_s + R_r k_r^2$$